



11th International Renewable Energy Storage Conference, IRES 2017, 14-16 March 2017,  
Düsseldorf, Germany

## Energy Performances of Open Sorption Reactor with Ultra-Low Grade Heat Upgrading for Thermochemical Energy Storage Applications

Oleksandr Skrylnyk<sup>a,\*</sup>, Emilie Courbon<sup>a</sup>, Nicolas Heymans<sup>a</sup>, Marc Frère<sup>a</sup>, Jacques Bougard<sup>b</sup>,  
Gilbert Descy<sup>b</sup>

<sup>a</sup>Department of Thermodynamics and Mathematical Physics, University of Mons, Boulevard Dolez 31, B-7000 Mons, Belgium

<sup>b</sup>Bureaux d'études solaires SPRL (BESOL), Street Griotte 2, B-5580 Rochefort, Belgium

---

### Abstract

The work discusses a problem of harvesting and upgrading of ultra-low grade heat with thermochemical energy storage technology for space and domestic water heating in residential area. The laboratory scale prototype, operating on the principle of an open packed bed sorption reactor and using moist air as a heat/mass transfer fluid, is experimented. The range of experimental air temperature was set to 17–40 °C, which corresponds to the typical range of domestic waste thermal energy. The tested sorbent was a salt-in-matrix composite material composed of a silica gel containing 43 wt.% of calcium chloride (CaCl<sub>2</sub>) salt. Hygrothermal behavior and energy performances of the prototype control volume filled with 245 g of material, representing the reactive front of a thermal wave, were analyzed at constant inlet hydration conditions (water vapor pressure of 12.5 mbar). The average temperature lift was recorded as 9–13 °C, representing the amplification of a supplied heat on 23% – 75% depending on the inlet temperature. The average specific thermal power inside the material bed was measured to be 168–267 W kg<sup>-1</sup>. The apparent energy density, based on the prototype control volume, ranged between 1.0 and 1.6 GJ m<sup>-3</sup>. Taking into account the heat of water vaporization, the coefficient of performance of the process was determined to be 0.96–1.57.

© 2017 The Authors. Published by Elsevier Ltd.

Peer-review under the responsibility of EUROSOLAR - The European Association for Renewable Energy.

*Keywords:* Thermochemical energy storage; ultra-low grade heat; composite material; open sorption; residential building;

---

\* Corresponding author. Tel.: +32-65-37-4238.

*E-mail address:* [oleksandr.skrylnyk@umons.ac.be](mailto:oleksandr.skrylnyk@umons.ac.be)

## 1. Introduction

Heat and electricity are the dominant types of energy end-used by buildings. The conversion of thermal energy into electricity [1, 2] and vice versa [3] is approved and perspective way for a large scale energy management. Such technological processes are based on various thermodynamic cycles and operate typically at temperatures from 500 °C to 1500 °C. The resulting high (>400 °C) and medium grade (200 °C – 400 °C) waste heat can be successfully recovered for the further reuse. However, harvesting low and ultra-low grade heat (up to 200 °C or <100 °C) is associated with a low economic viability [4]. Recently the potential of utilization of waste and ultra-low grade heat presented a live interest in different fields of thermal engineering applications, including combined power and heat generation (CHP) [5, 6], cascaded heating/cooling processes [7 – 11]. According to Rattner et al. [12], 20.3% of electricity usage and 12.5% of primary fuels could be replaced directly by a waste heat for end-use temperatures below 100 °C.

Space heating and domestic hot water preparation (SH&DHW) directly concern the vital spheres of human being and require usually temperature range between 30 °C and 65 °C. The recovery of a waste heat or the upgrade of an ultra-low grade heat to this temperature range meets particularly the objectives of energy saving and rational utilization in the future decarbonized society.

Ammar et al. [13] have studied the transportation of a low-grade heat over long distances from industries to domestic heat sinks. The authors have identified the economically viable distance of 30 – 40 km for the temperature as low as 80 °C using the chemical sorption technology from liquid solution of ammonia (NH<sub>3</sub>). The heating coefficient of performance (COP) was observed to be nearly 0.5. NH<sub>3</sub>/H<sub>2</sub>O chemical pair was selected for economic reasons. The authors accented though on risks associated with high concentrations of NH<sub>3</sub> in the air. Mazet et al. [14] investigated relevant solid/gas sorption cycles for low grade heat upgrading and transportation to the user site using a distant thermal source located over 10 km. Numerous well-known chemical pairs (chlorides and bromides as solid sorbents reacting either with NH<sub>3</sub> or with H<sub>2</sub>O as sorbate) have been evaluated. The described concept is typically adapted to the temperature range below 100 °C. The heat upgrading performances of investigated cycles resulted in COP bounded between 0.5 and 0.6. Li et al. [15] have proposed the thermochemical sorption heat transformer using reversible solid/gas reaction for the integrated energy storage and the low-grade thermal energy upgrading. The magnitude of the temperature upgrade could be adjusted in the range 19 °C – 152 °C according to identified chemical pairs (MnCl<sub>2</sub>–NaBr/NH<sub>3</sub>, MnCl<sub>2</sub>–CaCl<sub>2</sub>/NH<sub>3</sub> and NiCl<sub>2</sub>–SrBr<sub>2</sub>/NH<sub>3</sub>). The energy efficiency of low grade thermal storage ranged between 0.34 and 0.72. Yu et al. [16] suggested that the utilization of solid/gas reactive heat transformers, exploiting directly the low grade heat, is more reasonable compared to compression heat pumps based upon electricity, that was being derived from high grade thermal energy.

In order to improve the energy efficiency and economic effectiveness resulting from recovering a waste heat and upgrading an ultra-low grade heat to the end-use purposes, there is a need for energy storage [17]. Bao et al. [18] explored the simultaneous electric and thermal energy storage integrated cycle using the ultra-low grade heat with temperatures from 30 °C to 100 °C. The proposed principle uses MnCl<sub>2</sub>–CaCl<sub>2</sub>/NH<sub>3</sub> and CaCl<sub>2</sub>–NaBr/NH<sub>3</sub> as reactive chemical systems and is characterized as a highly efficient reversible chemisorption-to-power process with overall efficiency between 0.6 and 0.65 at 30 °C (source temperature). The thermal energy storage density of the integrated cycle was up 0.28 GJ m<sup>-3</sup>, while the electrical energy storage density was limited only by 0.02 GJ m<sup>-3</sup>. Zhao et al. [19] have designed the laboratory scale sorption heat storage prototype aiming to replace the conventional hot water storage tank in SH&DHW applications. The prototype was tested for energy charging at 85 °C and energy discharging at 40 °C as temperature conditions. The recovery process of ultra-low grade heat at 30 °C allowed lifting the energy density of the prototype by 50%, compared to initially used heat source at 18 °C without heat recovery. The applied material was the consolidated composite material (expanded graphite + 93 wt.% of LiCl) that reacted with H<sub>2</sub>O vapor. Lu et al. [10] have developed multi-step sorption cycles with temperature upgrading and thermal energy storage for solar heating and cooling purposes. The developed cycles were based upon LiCl/H<sub>2</sub>O working pair. The heat upgrading cycles shifted the source temperature by 50 °C – 60 °C. The discharging heat storage density arrived to 2.0 GJ m<sup>-3</sup> and provided COP of 0.61 – 0.64 for the temperature upgrading cycle. Liu et al. [20] have synthesized a novel thermal energy storage material (Wakkanai siliceous shale + 22.4 wt.% of CaCl<sub>2</sub>) to work in an open sorption system for ultra-low grade industrial waste heat recovery. The source air temperature was supplied at 25 °C to the prototype installation and the resulting temperature was upgraded greater than 40 °C. The developed system required

a low charging temperature (80 °C – 100 °C). The obtained energy density was 0.27 GJ m<sup>-3</sup> and the COP was found as 0.65 during the heat release.

Therefore, the thermochemical sorption process, driven by waste or ultra-low grade heat, can be successfully deployed in the building sector. The present work addresses the experimental investigation of performances of an open sorption packed bed reactor used as thermochemical energy storage (TCES) in residential buildings. The open sorption process was experimented through a laboratory scale apparatus. The ability to upgrade the ultra-low grade heat or to reuse the waste heat by newly synthesized composite material was particularly in focus of this study. Considering the increasing demand on low-temperature solutions for buildings, such materials and processes dealing with ultra-low heat storage, will significantly improve the efficiency of solar collectors arrays or CHP plants, as well as of heating networks and electricity grids.

## 2. Buildings and TCES technology: background and challenges

### 2.1. Opportunities of ultra-low grade heat upgrading in residential area with TCES technology

Air and water are obviously the main heat carrying fluids for building application. Thus, exhaust air from ventilation and hot wastewater/sewage evacuated from dwellings are ranked as the most typical sources of ultra-low grade heat. The energy demand by buildings depends on the energy class of housing and the installed equipment. The consumption of energy by buildings can be certainly decreased, but not completely eliminated. A building's occupancy requires a certain level of comfort, as well as includes domestic household services. Peaks of energy consumption often occur and the demand on energy can mismatch the heat supplying possibilities. The tightening regulation policies, especially on account of residential area, constantly reduce the amount of waste heat, but do not discard the quality. The resulting thermal waste energy is yet being discharged to the environment around the temperature range of human comfort sensations (15 °C – 30 °C). The efficiency and viability of waste heat recovering and upgrading depends on the available amount. On average, around 25% – 30% of thermal energy supplied to building is being evacuated by a ventilation system. Respectively, the share of energy drained off by a hot wastewater/sewage represents 15% – 30% of total building energy balance [21]. Frijns et al. [22] stated that the daily theoretical heat in wastewater living the house is 21.3 MJ per home. According to Forman et al. [23], the global residential waste heat amount below 100 °C reaches 10.952 PJ per year that represents 36% of share in total domestic rejected energy.

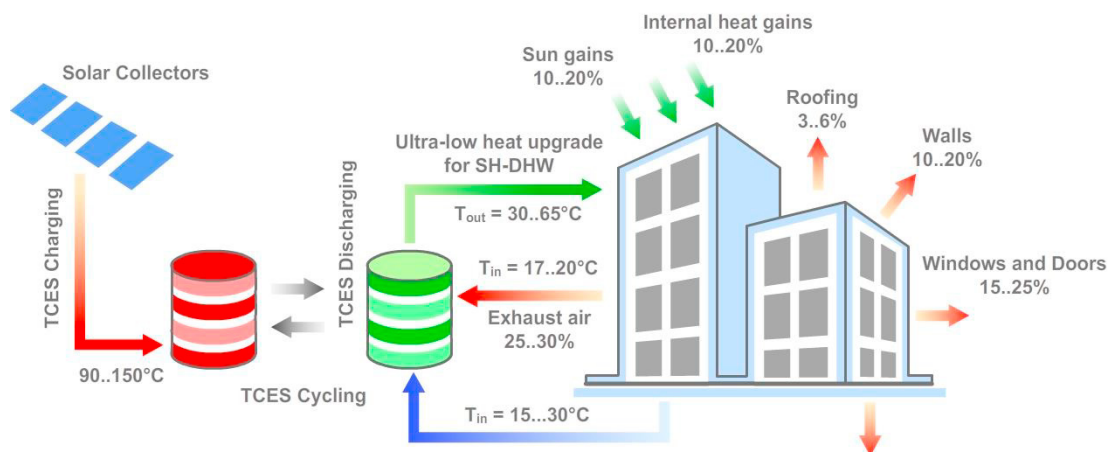


Fig. 1. Concept of on-site ultra-low grade heat upgrading process for SH&DHW in residential area by TCES plant. The data for heat losses are adapted from [21]. The concept suggests the time mismatch between building energy demand and solar collectors array productivity or peaks of energy demand occur. The sizing of TCES plant depends on the duration of charging and discharging cycle.

The TCES, using reversible solid/gas sorption reaction, is considered to be an advantageous heat storing and heat upgrading technology, due to a high energy density using solid sorbent (from 0.25 to 2.5 GJ m<sup>-3</sup> of storage material, that is 10 times higher than conventional DHW storage [24]), practical absence of side losses during long-term storage and its climate positive influences. The typical operation of a TCES plant involves the thermal energy charging (endothermic solid/gas reaction), storing and discharging (exothermic solid/gas reaction) stages, whereas the heat is recovered or upgraded to the necessary temperature levels during the discharging stage.

A number of conceptual solutions for the integration of TCES to buildings for SH&DHW purposes have been discussed in the literature. Skrylnyk et al. [25] have studied combined TCES configurations with heat recovering in an open sorption reactor. The proposed configurations were based upon air-to-water and warm air heating techniques. The energy efficiency for heat generation varied between 15% and 75% depending on the configuration. N'Tsoupkoe et al. [17] discussed a concept of cascaded TCES supplied by solar collectors or CHP plant. The concept was designed upon a closed sorption principle using heat recovery from condensation. The best energy efficiency was found as 65%. Hennaut et al. [26] have simulated a solar thermal combisystem integrating a closed sorption seasonal energy storage.

Fig. 1 presents an original concept of waste heat upgrading process by TCES plant in a building. The temperature of exhaust air is considered in the interval of 17 – 20 °C, while that of hot wastewater or sewage can vary from 15 °C to 30 °C. The building can be supplied by an array of solar collectors in case of on-site SH&DHW production or alternatively by a CHP plant for district SH&DHW applications. The TCES charging stage requires a higher level of temperatures than discharging temperatures (see Fig. 1). The upgrading performances of the supplied ultra-low grade heat to the end use thus depend on material (solid/gas chemical pair), thermodynamic cycle (single-step, multi-step or cascaded arrangement), TCES reactor design (open or closed sorption system), as well as on heat and mass transfer properties on macro- and component level inside the TCES reactor.

The illustrated processes [8 – 20] are designed on the grounds of either open or closed sorption systems. Multi-step and cascaded cycles provide a greater temperature lift than a single-step process. The open sorption reactor can be more versatile, compared to the closed sorption reactor, because: (i) it can be operated at the atmospheric conditions; (ii) no need of reactive gas storage (or rather limited need as gas condensate), thus the TCES can be more compact; (iii) heat and mass transfer is more effective when reactive gas is being transported by carrier gas (usually outside air). Abedin A. et al. [27] have illustrated that the overall system energy efficiency is 50% for closed sorption systems and 69% for open sorption processes. Both systems are nevertheless relevant and reliable for TCES design.

## 2.2. Materials for harvesting ultra-low grade heat

The methodology of solids screening, accented on SH&DHW boundary conditions and heat upgrade requirements, has been widely studied in literature [14, 16, 28 – 33]. The commonly selected candidate materials are inorganic salts (i.e. SrBr<sub>2</sub>, MgCl<sub>2</sub>, CaCl<sub>2</sub>, MgSO<sub>4</sub>, LiCl, MnCl<sub>2</sub>, NaBr etc.), zeolites, silica gel (SG). NH<sub>3</sub> and H<sub>2</sub>O vapors are of the most typical consideration among ecologically neutral reactive gases, due to a high affinity to the very wide family of solids [24]. The chemical pairs using H<sub>2</sub>O vapor are more often selected for SH&DHW applications. They can be used both in closed and open sorption systems. Moreover, H<sub>2</sub>O is the most available, non-toxic and cheap reactive component, since it is present in all vital spheres. On the contrary, chemical pairs working with NH<sub>3</sub> are considered to be reliable for heat upgrading processes with distant heat source and cooling applications. They are preferably implemented in thermodynamic sorption cycles isolated from ambient environment and human contact. For the use in open sorption TCES, we eliminated NH<sub>3</sub> compliant pairs from the further considerations.

Since the upgrade of ultra-low grade heat performs at relatively low discharging temperatures (15 °C – 30 °C), some chemical pairs based on hygroscopic salts (e.g. LiCl/H<sub>2</sub>O, CaCl<sub>2</sub>/H<sub>2</sub>O, SrBr<sub>2</sub>/H<sub>2</sub>O, MgSO<sub>4</sub>/H<sub>2</sub>O) are exposed to the deliquescence phenomenon, when the relative air humidity (R.H.) exceeds a certain threshold [31]. Besides, swelling and agglomeration are common problems for many hygroscopic inorganic salts. These phenomena significantly reduce the energy performances after several charging/discharging cycles. Moreover, the utilization of pure salts can cause severe corrosion of TCES parts. In order to overcome these shortcomings, especially for open sorption reactors with uncontrolled air humidity, composite materials can be synthesized using porous materials as host matrices [20, 31 – 33]. The host matrices and salts have different thermodynamic and physical properties. In addition, different sorption mechanisms take place in separate host matrices and salts. Thus the procedure of composite

materials synthesis tries to determine an optimal salt content in a given host matrix, so that the resulting hygrothermal performances would be as high as possible with regards to the phenomenological and operational restrictions.

### 3. Experiments with laboratory scale apparatus

#### 3.1. Tested material

To fulfill the research objectives, a composite material has been synthesized using  $\text{CaCl}_2$  (Caso® granules of 94 % of purity provided by Solvay) and silica gel porous matrix (Davisil® of grade 62 from Grace). The method of synthesis included [32]: (a) drying of SG particles in laboratory oven at 200 °C; (b) impregnation of SG particles from aqueous solution of 20 wt.% dissolved  $\text{CaCl}_2$ . The steps (a) and (b) have been consequently repeated, so that final impregnation rate of  $\text{CaCl}_2$  has reached 43 wt.%. The obtained SG +  $\text{CaCl}_2$  composite material has undergone the characterization of its fundamental thermodynamic properties. The tests with thermogravimetric and differential scanning calorimetric analysis (TGA/DSC setup from Setaram) showed 0.75  $\text{GJ m}^{-3}$  of energy storage density for bulk material and 1.02  $\text{MJ kg}^{-1}$  of energy storage capacity in temperature range between 30 and 80 °C at 12.5 mbar of water vapor pressure. The obtained bulk specific mass of material is 734  $\text{kg m}^{-3}$ . The measurements based on  $\text{N}_2$  sorption at 77 K (using BELSORP-max apparatus from BEL Japan Inc.) have recorded the decrease of pores volume from 1.06  $\text{cm}^3 \text{g}^{-1}$  (Davisil® SG matrix) to 0.38  $\text{cm}^3 \text{g}^{-1}$  (SG + 43 wt.% of  $\text{CaCl}_2$ ) after synthesis. No degradation of hygrothermal characteristics was observed during the stability tests with TGA/DSC (10 charging/discharging cycles in the mentioned above conditions). The isotherm data have been measured with dynamic sorption analyzer IGASorp from Hiden Isochema, see Table 1.

Table 1. Adsorption isotherm data for SG +  $\text{CaCl}_2$  (43 wt.%) composite material [32].

Temperature, $T_a$ (°C)	Water vapor pressure, $P_v$ (mbar)	Equilibrium water uptake, $x_e$ ( $\text{kg kg}^{-1}$ )
20	12.85	0.869
30	12.75	0.540
40	13.26	0.366
60	11.99	0.145
80	14.12	0.120

#### 3.2. TCES open sorption prototype

The schematic diagram of the designed laboratory scale prototype is illustrated on Fig. 2. The prototype was conceived to test the energy performances of solid granular sorbents at the medium scale (from 0.2 to 1 kg of bulk material). The heat and mass transfer fluid (reactive gas) is the moist air. Experimental setup consists of the sorption column, the humidification system and the dry air storage. The sorption column is mounted with three aluminum stacked cylindrical sections. The material can be loaded upon the circular sieve located at the bottom of the central section (reactive granular bed), whose cross-section area for air flow is 0.05  $\text{m}^2$ . The internal volume of central section is 4.5 l. The internal volume of upper (bed output) and lower (bed input) cylindrical sections is 6.1 l each. The input/output bed sections are thermally jacketed by overwrapped water-heated copper coils. The sorption column is equipped with three sets of four standard K-type thermocouples distributed at different locations of column sections. Two sets of four thermocouples are used to measure air temperature at the input/output of the granular bed. Other set of thermocouples measures directly the temperature inside the reactive granular bed. Each input/output column's section carries one air humidity probe HC2-P05 from Rotronic. The variations of bed mass during the sorption tests are measured in-situ by weighing balance (Signum® 1 from Sartorius).

The air humidification system is used to control the generation of the moist air from the dry air storage and is realized with Bronkhorst® fluid handling instruments, including controlled evaporator-mixer chamber (CEM), air and water flow meters (FG and FL connected to the data acquisition system). The temperature of the moist air is regulated to the desired level by switching the air pipes between the air heater or air cooler. The air heater is the electric resistance

of 1 kW and provides the regulation of air temperature above room temperature. The air cooler is the corrugated fine-wall metallic tube flooded in the cooling bath. The air cooler is active for the temperature range lower than room temperature. Although the air pipes are thermally isolated, the problem of heat losses still persists and the sorption column operates in the actual range of air temperatures between 12 and 72 °C. The CEM settings can be checked with one additional thermocouple and pressure transducer (GEFRAN TK series) placed at the column inlet.

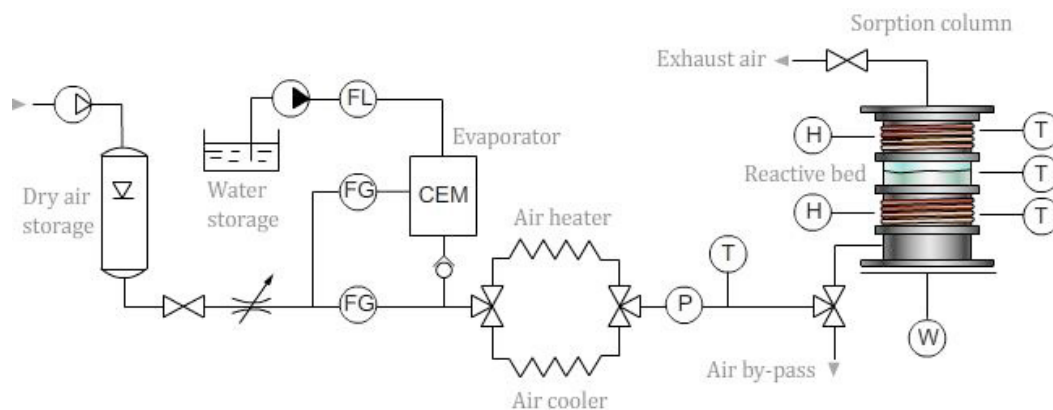


Fig. 2. Schematic diagram of laboratory setup: CEM is controlled evaporator-mixer, FG is gas flow meter, FL is liquid flow meter, P is pressure transducer, T is temperature sensor, H is humidity sensor and W is weighing balance.

The dry air storage uses a tank of 132 l of capacity from the commercial compressor/dyer package DAP2000B from General Air Products, Inc. The adjustment of the air pressure, with regards to the pressure drop in the air pipes, is made by pressure regulator situated at the outlet of the dry air storage tank. The experimental data from all sensors are collected by the CompactDAQ® data acquisition system from National Instruments™ Corp.

### 3.3. Description of experimental procedure

The experimental procedure was developed with regards to the constant and stable inlet conditions (air temperature and air R.H.). This approach relates process performances at component size (material + reactor) to the equilibrium characteristics of material alone. The procedural steps are described below.

Each experiment preceded by material sample conditioning: (i) drying in the laboratory oven at 150 °C during 24 h; (ii) cooling down in the tight recipient to the room temperature; (iii) checking the residual water content  $x_0$  with moisture analyzer (model HE73 from Mettler Toledo). The mass of anhydrous material sample  $m_{s,0}$  can be thus established using  $x_0$  to have the common reference.

Preparation of the prototype to experiment: (i) setting the air humidification system to the targeted experimental conditions; (ii) running empty column in the desired conditions during 40 minutes to reach the stable temperature and air R.H. values; (iii) adjusting the CEM settings, if the deviations of the targeted conditions are observed. These manipulations allow also the metallic air pipes and column sections to heat up (or to cool down), so any heat losses to the environment remain constant.

Starting and running the experiment: (i) switching the column inlet to the air by-pass position; (ii) loading the dehydrated and cooled material sample homogeneously on the sieve; (iii) switching back the valve to start the experiment. When material is being loaded to the column, it contacts shortly with the ambient air. We concluded nevertheless that the contact time (<3 min) did not cause any considerable effect and could be neglected compared to the overall experimental time (>4 hours).

The hygrothermal behavior of material and energy performances of TCES prototype were studied from the point of view of advancement of reaction front  $y_z(t)$  in a prototype control volume  $V_c$ . In a typical packed bed column, the bed temperature  $T_b$  decreases gradually in the direction of the air flow  $\dot{m}_a$  from column inlet to outlet as far as the hydration reaction approaches to equilibrium conditions  $x_e$ . The location of the reaction front  $y_z(t)$  progressively

displaces and follows the air flow stream lines. Therefore, the overall state of charge/discharge in the reactive granular bed can be considered as a sum of lumped reactive layers with equal heights  $h_z$ . The ratio of SG/moist air heat conductivities ( $\lambda_s/\lambda_a \sim 10$ ) is so that the Biot number  $Bi < 1.0$ . In this case, the temperature gradient inside the individual reactive layer is negligible  $\nabla_z T_b = 0$  and the measured bed temperature at the location of reaction front  $y_z(t)$  will determine the outlet air temperature  $T_b \cong T_{a,out} (\pm \Delta T_a)$  as inlet condition for the next layer. The temperature lift  $\Delta T_u = T_b - T_{a,in}$  within the reactor upscaling is limited by the hygrothermal behavior of an individual layer of height  $h_z$ .

The sample mass needed to represent a reaction front is given as  $m_s = \rho_{s,b} \cdot A_b \cdot h_z$ , where  $A_b$  is a column cross-section area for air flow. Measuring in-situ the variation of sample weight  $\Delta m_s(t)$  and using isotherm data  $x_e$  enables calculating the reaction advancement:

$$y_z(t) = \frac{x(t) - x_0}{\Delta x_e} \quad (1)$$

Where  $x(t) = \Delta m_s(t)/m_{s,0}$  is the water uptake and  $\Delta x_e = x_e - x_0$  is the loading lift. The specific thermal power produced during the advancement of reaction is given as:

$$\dot{Q}(y, t) = \frac{\dot{m}_a C_{P,a}}{m_{s,0}} (\langle T_b(y, t) \rangle_z - T_{a,in}) \quad (2)$$

Here  $\langle T_b(y, t) \rangle_z$  represents the average temperature measured inside the reactive bed layer of height  $h_z$ . The reaction kinetics can be deduced from the bed energy balance, when  $dT_b(y, t)/dt = 0$ , by following relation:

$$k_b = \frac{\dot{Q}_{max}(y)}{(1 - y)\Delta x_e \cdot \Delta H_s^0} \quad (3)$$

Where  $\Delta H_s^0$  is the hydration reaction enthalpy. The energy storage capacity related to the advancement of reaction is defined as follows:

$$E_M = \int_0^t \dot{Q}(y, t) dt \quad (4)$$

The prototype control volume  $V_c$  represents the volume of individual reactive layer for the advancement of reaction front with a height  $h_z$ . It is defined as  $V_c = A_b \cdot h_z$ . The energy storage density of reactive layer can be evaluated as:

$$E_V = \frac{m_{s,0}}{V_c} \cdot E_M \quad (5)$$

The thermal coefficient of performance related to the use of the prototype's humidification system is given by:

$$COP = \frac{E_M}{Q_{ev}} \quad (6)$$

Where  $Q_{ev}$  is the amount of energy required for water vaporization. This energy can be found as:

$$Q_{ev} = \int_0^t \frac{\dot{m}_w(t)}{m_{s,0}} \Delta H_{ev} dt \quad (7)$$

With  $\dot{m}_w$  is water flow rate set to CEM unit and  $\Delta H_{ev}$  is the standard water vaporization enthalpy. The relations (1 – 7) can be used for reactor upscaling. The ability of thermal power delivery by TCES prototype decreases in time during the discharging due to the reaction saturation. The residual thermal power, defined by the temperature lift  $\Delta T_u$ , may not be sufficient for the practical use, thus not all energy storage density is usable. Therefore, the determination of a reasonable discharging level  $y$  of storage and associated therein energy storage density  $E_V(y)$  is necessary for optimization of discharging/charging cycle of real scale TCES system.

#### 4. Experimental results and discussion

The experiments were run at constant inlet conditions in the temperature range between 17 and 40 °C, imitating thus the upgrade of the ultra-low grade heat with SG + CaCl<sub>2</sub> (43 wt.%) composite during TCES discharging operation. The implementation of the measurement method described by (1 – 7) was possible for granular shallow

beds with the heights of  $0.7 \leq h_z \leq 1.0$  cm. The required material sample mass was 245 g. The control volume  $V_c$  was thus 0.5 l. The experimental air volume flow rate, at which  $Bi < 1.0$ , was adopted as  $215 \text{ l min}^{-1}$  and the air velocity through the column empty section was  $0.073 \text{ m s}^{-1}$ . The targeted air R.H. at the column inlet was chosen as 50% at  $20^\circ\text{C}$  of air temperature, corresponding to 12.5 mbar of water vapor pressure. Several samples were used for studies. The experimental conditions are listed in Table 2.

Table 2. Experimental conditions set for laboratory prototype at constant air flow rate of  $215 \text{ l min}^{-1}$  and targeted air R.H. 50% at  $20^\circ\text{C}$ .

Experiment designation	Anhydrous sample, $m_{s,0}$ (g)	Inlet air temperature, $T_{a,in}$ ( $^\circ\text{C}$ )	Inlet water vapor pressure, $P_{v,in}$ (mbar)	Expected equilibrium, $\hat{x}_e$ ( $\text{kg kg}^{-1}$ )
DCH-17C	246.16	17.54	12.30	0.990
DCH-20C	244.76	20.89	13.26	0.889
DCH-30C	244.58	30.75	11.84	0.489
DCH-40C	245.92	40.23	13.13	0.381

The average residual water content in each sample after drying was  $x_0 = 2.9 \times 10^{-3} \text{ kg kg}^{-1} \pm 5.1\%$ . The expected  $\hat{x}_e$  values were calculated applying the polynomial extrapolation of equilibrium data from Table 1.

#### 4.1. Hygrothermal behavior of samples

The temperature lifts  $\Delta T_u$  recorded inside the granular beds during hydration experiments and the outlet water vapor pressures are shown on Fig. 3.

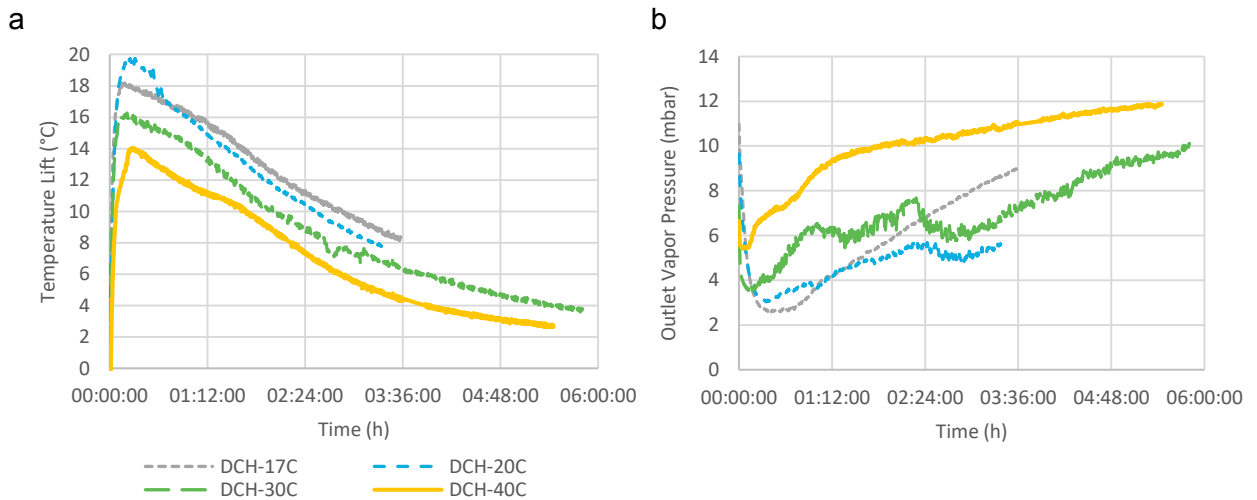


Fig. 3. Hygrothermal behavior of samples during experiments with different inlet air temperatures: (a) temperature lifts of granular beds and (b) outlet water vapor pressures. The temperature lift is found as the difference between average bed temperature and inlet air temperature.

It has to be noted that the duration of experiments was not the same due to material wetting followed by agglomeration of samples. The agglomeration was observed for water uptakes  $>0.25 \text{ kg kg}^{-1}$ , except DCH-40C test. The tests DCH-17C and DCH-20C had to be stopped after  $\sim 3 \text{ h } 20 \text{ min}$  because of significant wetting of samples. The fast rise of the outlet water vapor pressure for DCH-17C test (see Fig. 3b) is not related to high kinetics, but rather to the formation of air passages through the agglomerated layer.

The maxima and minima values of temperature lifts and pressures on Fig. 3 correlate well with adsorption isotherm data from Table 2 and so far the heat generation capacity intensifies with the growth of equilibrium uptake. The evolution of heat upgrading performances can be better observed on the plots of bed temperature lift  $\Delta T_u$  (Fig. 3a),



instead of measured  $T_b$ . The measurements showed that the bed temperature  $T_b$  was sharply rising and the temperature lift  $\Delta T_u$  reached its peak values during the first 20 minutes in all experiments. At the same time, the outlet water vapor pressures dropped downwards the minima values (Fig. 3b).

The heat upgrading capacities of the used material thus depend on the supplied air temperature. For the time span between 0 h 20 min and 3 h 20 min, the average temperature lifts (Fig. 3a) are 13.23 °C (DCH-17C), 13.35 °C (DCH-20C), 11.21 °C (DCH-30C) and 9.32 °C (DCH-40C), meaning the amplification of the ultra-low grade heat ( $\propto \Delta T_u/T_{a,in}$ ) on 75.4%, 63.9%, 36.5% and 23.2% in respective order of tests. The front of  $\Delta T_u$  curves has the same shape for all tests that is obviously related to the heat transfer properties of SG + CaCl<sub>2</sub> material. The parallel shift of temperature curves indicates that the heat transfer remained the same for the used constant air flow rate and air R.H. The average velocity of heat release attenuation (the slope of temperature curves) is 3.27 °C h<sup>-1</sup> ±6.5% for all tests.

#### 4.2. Evaluation of energy performances

Energy performances after all tests were evaluated with equations (1 – 7). The main results are presented in Table 3. The plots of specific thermal powers  $\dot{Q}$  and COPs as functions of reaction advancement  $y_z$  are shown on Fig. 4. The discharging energy performances are correlated with water uptake lifts  $\Delta x = x(t_{tc}) - x_0$ , with  $t_{tc} = 3$  h 20 min. The recorded values of  $\Delta x$  (Table 3) are proportionally inversed to the experimental air inlet temperatures (Table 2), so that the higher  $\Delta x$  correspond to the lower  $T_{a,in}$ .

The discharging energy performances are calculated for non-equilibrium conditions of tested samples, when  $y_z < 100\%$ . Reaching the equilibrium uptakes, as expected (Table 2), may be seen as unreasonable in real operating conditions, because: (i) the agglomeration of material for relatively low  $T_{a,in}$  temperatures ( $\leq 30$  °C) is still an issue; (ii) the generated thermal power dramatically decreases (diminishment on 70 – 80% of peak power) after the threshold of 65% (or  $\sim 2/3$ ) of reaction advancement (see Fig. 4a). Besides, the COP approaches to 1.0, meaning that the power spent for water vaporization is equal to the generated thermal power by TCES prototype (see Fig. 4b).

Table 3. Discharging energy performances of SG + CaCl<sub>2</sub> (43 wt.%) samples at constant air flow rate of 215 l min<sup>-1</sup> and targeted air R.H. 50% at 20°C on the time span of 3 h 20 min.

Experiment designation	$\Delta x$ (kg kg <sup>-1</sup> )	$y_z$ (%)	Average $\dot{Q}$ (W kg <sup>-1</sup> )	$E_M$ (MJ kg <sup>-1</sup> )	$E_V$ (GJ m <sup>-3</sup> )	COP
DCH-17C	0.418	44	267	3.19	1.57	1.57
DCH-20C	0.425	56	259	3.11	1.52	1.45
DCH-30C	0.305	62	211	2.54	1.24	1.39
DCH-40C	0.183	60	168	2.05	1.01	0.96

It can be though remarked that the measured energy storage capacities and densities from Table 3 are quite high, compared to the TGA/DSC measurements. This is mostly due to the dehydration temperatures, since TGA/DSC tests have been performed in a narrower temperature range (between 30 and 80 °C) and the experimented samples have been dehydrated at 150 °C. The flat plate glazed thermal collectors + DHW storage tank is a most typical configuration for a domestic thermal system in SH&DHW applications and is adapted for 80 °C as working temperature. The evacuated tube thermal collectors can perform at higher temperatures than 120 °C and require less roofing surface than flat plate collectors. Therefore, the evacuated tube collectors (or CHP plant) + TCES stands as more efficient solution to valorize the thermal energy storage. The boost of performances for the upgrade of ultra-low grade heat (in terms  $\Delta T_u$ ) with the open sorption TCES is possible in two cases: (a) intensification of air moistening process; (b) increase of charging temperature. Both ways are nevertheless valuable and a heat source is required. The energy storage density (and capacity) is of course an important characteristic of TCES, but independently of this parameter, the optimal functioning of TCES, especially as a heat transformer for waste heat recovery, relies on thermal power and COP characteristics.

For the discharging conditions used in the experiments, the maxima values of specific thermal powers  $\dot{Q}$  (Fig. 4a) and COP (Fig. 4b) occur at different reaction advancement levels. The  $\dot{Q}(y)$  datasets of tests DCH-17C and DCH-20C overlap and their  $COP(y)$  are very similar. This is due to the proximity of experimental  $T_{a,in}$  temperatures (Table

2). The specific thermal powers for these two tests reach their peak values (351 and 386 W kg<sup>-1</sup>) already at the  $y_z \approx 5\%$ . The maxima values of COP, namely 2.06 and 1.96, occur at  $y_z = 12\%$  for DCH-17C test and respectively at  $y_z = 8\%$  for DCH-20C.

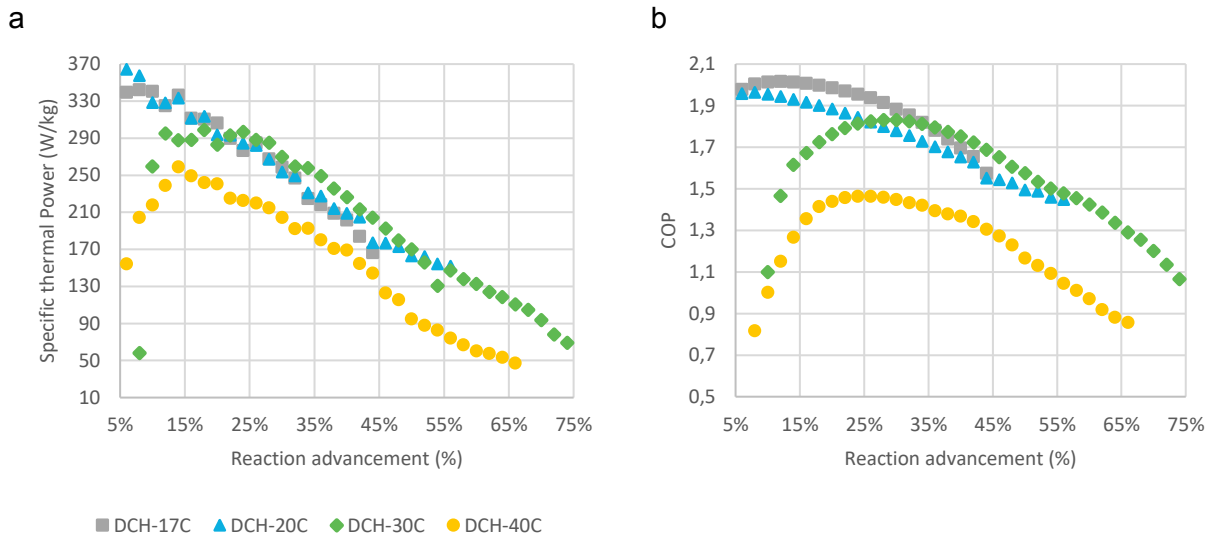


Fig. 4. Performances plots: (a) specific thermal power and (b) COP as functions of reaction advancement.

Both  $\dot{Q}(y)$  and  $COP(y)$  datasets of the DCH-30C test seem to be a continuation of DCH-17C and DCH-20C plots in the region of  $y_z \geq 55\%$ . Due to progressing wetting issues of samples, the tests DCH-17C and DCH-20C could not be carried out beyond 56% of  $y_z$ . The datasets of the test DCH-30C achieve the peak values of  $\dot{Q}_{max} = 299 \text{ W kg}^{-1}$  and  $COP_{max} = 1.83$  at  $y_z = 18\%$  and respectively at  $y_z = 30\%$ . The performances of datasets for the test DCH-40C are situated lower than for other tests. The maxima values of  $\dot{Q}_{max} = 259 \text{ W kg}^{-1}$  at  $y_z = 14\%$  and  $COP_{max} = 1.46$  at  $y_z = 26\%$ .

In all experimental cases, the attenuation of  $\dot{Q}(y)$ , relative to maxima values, is quasi linear and has, on average, the slope of  $4.27 \text{ W kg}^{-1} \%^{-1} \pm 4.3\%$ . The profiles of  $COP(y)$  are convex curves and have no common degree of curvature. The kinetic rate  $k_b$  was determined with the relation (3) using the corresponding  $\dot{Q}_{max}(y)$  data from Fig. 4a. The results are presented in Table 4. The inlet air temperature has a direct effect on reaction kinetics, which grows as far as the inlet setpoint temperature increases (see  $T_{a,in}$  values in Table 2).

Table 4. Kinetic rate of SG + CaCl<sub>2</sub> (43 wt.%) material under constant hydration conditions. The hydration reaction enthalpy  $\Delta H_s^0$  is 2757 KJ kg<sup>-1</sup>.

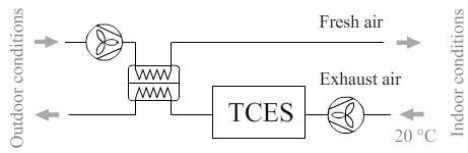
Experiment designation	$k_b$ (s <sup>-1</sup> )
DCH-17C	$1.3 \cdot 10^{-4}$
DCH-20C	$1.6 \cdot 10^{-4}$
DCH-30C	$2.7 \cdot 10^{-4}$
DCH-40C	$2.9 \cdot 10^{-4}$

The discharging energy performances have been calculated for the so-called lossless situation of the shallow granular bed. The heat volumetric losses of the upper column section were calculated and they ranged between 1.23 and 5.25 W l<sup>-1</sup> depending on the bed temperature lift. The volumetric heat losses can be regarded as dissipation of heat during the transportation of warm air along the air ducts. With account of the heat dissipation, the energy density and the COP drop dramatically down on 36% – 72%. Therefore, the heat losses are the substantial problem that reduces

the thermal upgrading ability (in terms of average temperature lift) on 15% – 32% and have to be accounted for real system sizing.

Regarding the proximity of datasets depicted on Fig. 4, we can link the thermal waste source and the performances of TCES. The proximity of those datasets signifies that the TCES exhibits similar heat upgrading performances for the exhaust air and the cold wastewaters/sewage at 17 °C and 20 °C. In this case, TCES can work as a heat transformer in a single-stage cycle for heating applications with warm air. The results from Table 3 can be applied to size TCES system for a specific case as follows. Consider a dwelling with yearly space heating demand ~5.4 GJ, which might represent a standard passive house with 100 m<sup>2</sup> of living surface. The TCES sizing assessment is presented in Table 5, assuming that the house is equipped with air-to-air heat recovery unit and TCES is integrated to the exhaust air conditioning duct.

Table 5. Example of TCES sizing for specific case study.

System configuration	Yearly energy demand (GJ)	Required heat power (W)	Overall system efficiency (%)	Single bed mass (kg)	Total material storage mass (kg)
	5.4	1500	90	6.44	1930
			85	6.81	2043
			80	7.24	2170
			70	8.27	2480

Concerning the temperature levels of 30 °C and 40 °C, they can be drawn from the hot wastewater. The TCES has to be integrated in the recirculation circuit for DHW provision system. The space heating with higher temperature shifts than shown on Fig. 3a would require the implementation of a cascaded cycle.

## 5. Conclusions

Composite material SG + CaCl<sub>2</sub> (43 wt.%) was studied to generate the thermal power from the ultra-low grade heat source, using moist air as a heat carrier fluid. Experiments were carried out under reference conditions in the laboratory size set-up whose configuration is closed to the real scale energy storage system. The experimental procedure was developed in order to link the process energy performances to the hygrothermal response of the shallow granular bed with a layer thickness up to 0.01 m.

Specific thermal power (168 W kg<sup>-1</sup> – 267 W kg<sup>-1</sup>), thermal COP (0.96 – 1.57), energy storage capacity (2.05 MJ kg<sup>-1</sup> – 3.19 MJ kg<sup>-1</sup>) and density (1.01 GJ m<sup>-3</sup> – 1.57 GJ kg<sup>-3</sup>), as well as average heat upgrading ability (23% – 75%) have been obtained. Under the given experimental conditions, the average temperature lift of material layer ranged between 9.3 °C and 13.4 °C. The obtained results represent the single-stage heat upgrading operation.

Better heat upgrading performances were found for the low temperature heat source (up to 30 °C) due to the adsorption isotherm data. However, the prolonged hydration with temperature below 30 °C may cause material wetting and agglomeration, thus the recommended reaction advancement level is limited between 50% and 60%.

The analysis of experimental results and their application to the specific case shows that this material is suitable for the use in domestic thermal applications with waste heat recovery, especially from exhaust air or drain wastewater. The heat upgrading operation for the heat source temperature higher than 30 °C is reasonable with multi-stage (for example resorption) or cascaded cycles.

## Acknowledgements

This work was funded by the European Commission within the EU's Seventh Framework Program for Research (FP7) under the grant agreement reference ENER/FP7EN/295775/"SOTHERCO".

## References

- [1] Widmann C., Lödige D., Toradmal A., Thomas B. Enabling CHP units for electricity production on demand by smart management of the thermal energy storage. *Applied Thermal Engineering* 2017;114:1487-1497.
- [2] Tanaka Y., Mesfun S., Umeki K., Toffolo A., Tamaura Y., Yoshikawa K. Thermodynamic performance of a hybrid power generation system using biomass gasification and concentrated solar thermal process. *Applied Energy* 2015; 160:664 - 672.
- [3] Estermann T., Newborough M., Sterner M. Power-to-gas systems for absorbing excess solar power in electricity distribution networks. *International Journal of Hydrogen Energy* 2016; 41:13950-13959.
- [4] Walsh C., Thornley P. Barriers to improving energy efficiency within the process industries with a focus on low grade heat utilisation. *Journal of Cleaner Production* 2012; 23:138-146.
- [5] McDaniel B., Kosanovic D. Modeling of combined heat and power plant performance with seasonal thermal energy storage. *Journal of Energy Storage* 2016; 7:13-23.
- [6] Chaiyat N., Kiatsiriroat T. Analysis of combined cooling heating and power generation from organic Rankine cycle and absorption system. *Energy* 2015; 91:363-370.
- [7] Zhao X., Fu L., Wang X., Sun T., Wang J., Zhang S. Flue gas recovery system for natural gas combined heat and power plant with distributed peak-shaving heat pumps. *Applied Thermal Engineering* 2017; 111:599-607.
- [8] Li Y., Fu L., Zhang S., Zhao X. A new type of district heating system based on distributed absorption heat pump. *Energy* 2011; 36:4570-4576.
- [9] N'Tsoukpoe K.E., Mazet N., Neveu P. The concept of cascade thermochemical storage based on multimaterial system for household applications. *Energy and Buildings* 2016; 129:138-149.
- [10] Lu Z., Wang R., Gordeeva L. Novel multi-step sorption reaction energy storage cycles for air conditioning and temperature upgrading. *Energy* 2017; 118:464-472.
- [11] Najjar Y.S.H. Enhancement of performance of gas turbine engines by inlet air cooling and cogeneration system. *Applied Thermal Engineering* 1996; 16:163-173.
- [12] Rattner A.S., Garimella S. Energy harvesting, reuse and upgrade to reduce primary energy usage in the USA. *Energy* 2011; 36:6172-6183.
- [13] Ammar Y., Chen Y., Joyce S., Wang Y., Roskilly A.P., Swailes D. Evaluation of low grade heat transport in the process industry using absorption process. *Applied Thermal Engineering* 2013; 53:217-225.
- [14] Mazet N., Luo L., Stitou D., Berthiaud J. Feasibility of long-distance transport of thermal energy using solid sorption process. *International Journal of Energy Research* 2010; 34:673-687.
- [15] Li T., Wang R., Kiplagat J.K. A target-oriented solid-gas thermochemical sorption heat transformer for integrated energy storage and energy upgrade. *AIChE Journal. Thermodynamics and Molecular-Scale Phenomena* 2013; 59:1334-1347.
- [16] Yu Y.Q., Zhang P., Wu J.Y., Wang R.Z. Energy upgrading by solid-gas reaction heat transformer: A critical review. *Renewable and Sustainable Energy Reviews* 2008; 12:1302-1324.
- [17] N'Tsoukpoe K.E., Osterland T., Opel O., Ruck W. Cascade thermochemical storage with internal condensation heat recovery for better energy and exergy efficiencies. *Applied Energy* 2016; 181:562-574.
- [18] Bao H., Ma Z., Roskilly A.P. Integrated chemisorption cycles for ultra-low grade heat recovery and thermo-electric energy storage and exploitation. *Applied Energy* 2016; 164:228-236.
- [19] Zhao Y.J., Wang R.Z., Li T.X., Nomura Y. Investigation of a 10 kWh sorption heat storage device for effective utilization of low-grade thermal energy. *Energy* 2016; 113:739-747.
- [20] Liu H., Nagano K., Sugiyama D., Tagawa J., Nakamura M. Honeycomb filters made from mesoporous composite material for an open sorption thermal energy storage system to store low-temperature industrial waste heat. *International Journal of Heat and Mass Transfer* 2013; 65:471-480.
- [21] WASENCO. Wastewater heat recovery. <http://wasenco.com/en/wastewater-heat-recovery/>. [Accessed 2 Decembre 2016].
- [22] Frijns J., Hofman J., Nederlof M. The potential of (waste)water as energy carrier. *Energy Conversion and Management* 2013; 65:357-363.
- [23] Forman C., Muritala I.K., Pardemann R., Meyer B. Estimating the global waste heat potential. *Renewable and Sustainable Energy Reviews* 2016; 57:1568-1579.
- [24] Cabeza L.F., Solé A., Barreneche C. Review on sorption materials and technologies for heat pumps and thermal energy storage. *Renewable Energy* 2017; 110:3-39.
- [25] Skrylnyk O., Henry M., Courbon E., Heymans N., Frère M., Tanguy G., Papillion P., Bougard J., Beeckmans M., Descy G. Evaluation of the performance criteria of combined thermo-chemical energy storage systems for building applications. (EuroSun 2014) International Conference On Solar Energy And Buildings, Aix-les-Bains, France, 2014.
- [26] Hennaut S., Thomas S., Davin E., Skrylnyk O., Frère M., André P. Dynamic simulations of solar combisystems integrating a seasonal sorption system: Influence of the combisystem configuration. *Strojarsstvo* 2012; 54:433-440.
- [27] Abedin A.H., Rosen M.A. Closed and open thermochemical energy storage: Energy- and exergy-based comparisons. *Energy* 2012; 41:83-92.
- [28] Courbon E., Skrylnyk O., Hennaut S., André P., Frère M. Procédure simple pour estimer les capacités de stockage de chaleur des systèmes solide/gaz: Application au stockage d'énergie solaire dans les bâtiments [fr]. *Récents Progrès en Génie des Procédés* 2011; 101.
- [29] N'Tsoukpoe K., Schmidt T., Rammelberg H., Watts B., Ruck W. A systematic multi-step screening of numerous salt hydrates for low temperature thermochemical energy storage. *Applied Energy* 2014; 124:1-16.
- [30] Visscher K., Veldhuis J. Comparison of candidate materials for seasonal storage of solar heat through dynamic simulation of building and renewable energy system. (IBPSA 2005) 9th International IBPSA Conference on Building Simulation, Montréal, Canada, 2005.
- [31] Zhao Y.J., Wang R.Z., Zhang Y.N., Yu N. Development of SrBr<sub>2</sub> composite sorbents for a sorption thermal energy storage system to store

- low-temperature heat. *Energy* 2016; 115:129-139.
- [32] Courbon E. Étude du stockage d'énergie thermique d'origine solaire par réaction thermochimique [fr]. PhD thesis, Mons, Université de Mons, Belgium, 2016.
- [33] Casey S.P., Aydin D., Riffat S., Elvins J. Salt impregnated dessicant matrices for open thermochemical energy storage - Hygrothermal cyclic behaviour and energetic analysis by physical experimentation. *Energy and Buildings* 2016; 92:128-139.